Materials Science Forum Vols. 524-525 (2006) pp. 639-644
online at http://www.scientific.net
© (2006) Trans Tech Publications, Switzerland

In Situ Neutron Diffraction Study on the Mechanical Behavior of an Ultra-Fine-Grained Steel

K. Tao[1,a], H. Choo[1,2,b], H. Li[1,c], B. Clausen[3,d], D. W. Brown[4,e], J. E. Jin[5,f], and Y. K. Lee[5,g]

[1]Department of Materials Science and Engineering, The University of Tennessee, Knoxville, TN 37996, USA
[2]Materials Science and Technology Division, Oak Ridge National Laboratory, Oak Ridge, TN, 37831, USA
[3]Los Alamos Neutron Science Center, Los Alamos National Laboratory, Los Alamos, NM 87545, USA
[4]Materials Science and Technology Division, Los Alamos National Laboratory, Los Alamos, NM 87545, USA
[5]Department of Metallurgical Engineering, Yonsei University, Seoul, 120-749, Korea
[a]ktao@utk.edu, [b]hchoo@utk.edu, [c]hqli@utk.edu, [d]clausen@lanl.gov, [e]dbrown@lanl.gov, [f]chean76@hanmail.net, [g]yklee@yonsei.ac.kr

Keywords: Martensitic transformation, Ultra-fine-grained steel, Neutron diffraction, Lattice strain

Abstract. The martensitic phase transformation in an ultra fine grained (UFG) TRIP (transformation induced plasticity) steel with combination of high strength and high elongation was investigated during room temperature tensile test using *in situ* neutron diffraction. Two types of specimens, namely coarse grained (grain size of about 50 μm) and ultra-fine-grained (grain size of about 350 nm) specimens were examined. The lattice strain evolution of the austenite and martensite phases was observed and the load partitioning between the phases was identified.

1. Introduction

Nanocrystalline and UFG materials have received extensive attention in recent years. It is well known that the strength can be dramatically enhanced with the decreasing grain size based on the Hall-Petch relationship. Therefore, grain refinement is technically attractive for the production of stronger materials. The recent development of the severe plastic deformation (SPD); such as equal channel angular pressing (ECAP), accumulative roll bonding, and high pressure torsion; can refine the coarse grain to the nanoscale [1-4]. However, the high yield strength is usually achieved at the expense of the ductility, as there is little uniform elongation after yielding due to the lack of strain hardening. Based on Hart's instability criterion [5], for a material with high yield stress (e.g., nano- or UFG materials), it is necessary for a large strain hardening to be present to maintain the uniform elongation before the localized deformation that leads to necking and the final failure of the material. The strain hardening process is accompanied by the accumulation and interaction of the dislocations. However, the UFG metals usually have a high initial dislocation density that is introduced during the processing of the material through the SPD. Therefore, the saturation of the dislocation density results in very low strain hardening rate and hence, poor ductility [6].

However, in the case of UFG TRIP steel, the martensitic phase transformation can provide another source of strain hardening. The replacement of the austenite by the martensite phase increases the strain hardening rate and delays the strain localization. The effective prevention of necking leads to a significant increase of the uniform elongation. Meanwhile, the volume expansion that accompanies the transformation also contributes to the ductility improvement [7].

In this paper, we present the neutron diffraction measurement results of the UFG TRIP steel [8-9] to provide a microscopic understanding of the transformation and deformation behavior.

All rights reserved. No part of contents of this paper may be reproduced or transmitted in any form or by any means without the written permission of the publisher: Trans Tech Publications Ltd, Switzerland, www.ttp.net. (ID: 128.165.83.86-20/11/06,17:09:31)

2. Experimental details

The material selected for this study is Fe-Cr-Ni-Mn steel with a nominal composition (in weight percent) of 10%Cr, 5%Ni, 8%Mn, and balance Fe (with 0.1%C). The ingot, prepared using a high frequency vacuum induction furnace, was hot-rolled to the plates of 10 mm thick and solution treated at 1200 °C for 30 min. The initial solution-treated plate (γ–fcc phase with an average grain size of about 50 μm) was cold rolled with about 75% thickness reduction and the γ phase transformed into α′ (bcc) phase. Then, the plate was annealed at 640 °C (10 °C higher than the reverse transformation finish temperature A_f) for 10 min to induce the reverse transformation of the mechanically induced α′ back to γ. After the reverse transformation, the ultra-fine-grained (UFG) austenite (γ) with an average grain size of about 350 nm was obtained. The detailed description of the material preparation is available in the literature [8-9].

The room-temperature tensile tests and *in situ* neutron diffraction measurements for the coarse grained (CG) and the ultra fine grained (UFG) samples were performed using the SMARTS instrument at Los Alamos Neutron Science Center [10]. At SMARTS, the tensile loading axis was oriented at 45° relative to the incident beam with the scattering angle fixed at $2\theta = \pm 90^{\circ}$ for two detector banks. This scattering geometry allows the simultaneous measurements of the lattice strains and changes in the diffraction peak intensities parallel (axial) and perpendicular (transverse) to the loading axis. More details about the in situ loading neutron diffraction measurements can be found in the literature [11-12].

The lattice parameters, which are used for the lattice strain calculation, can be obtained by the Rietveld analysis of the measured diffraction spectra using the General Structure Analysis System (GSAS) [13].

3. Results and discussion

3.1. Macroscopic mechanical behavior

The tensile engineering stress-strain curves recorded during the neutron measurements are presented in Fig. 1. Nominal load of 20 MPa was used as the stress-free reference. The serrations (decreases in the load) in the stress-strain curve are due to the stress relaxation while holding the specimen at constant position for diffraction pattern collection for about 20 min. A few unloads were also performed to measure the residual lattice strains (not discussed here). The UFG specimen

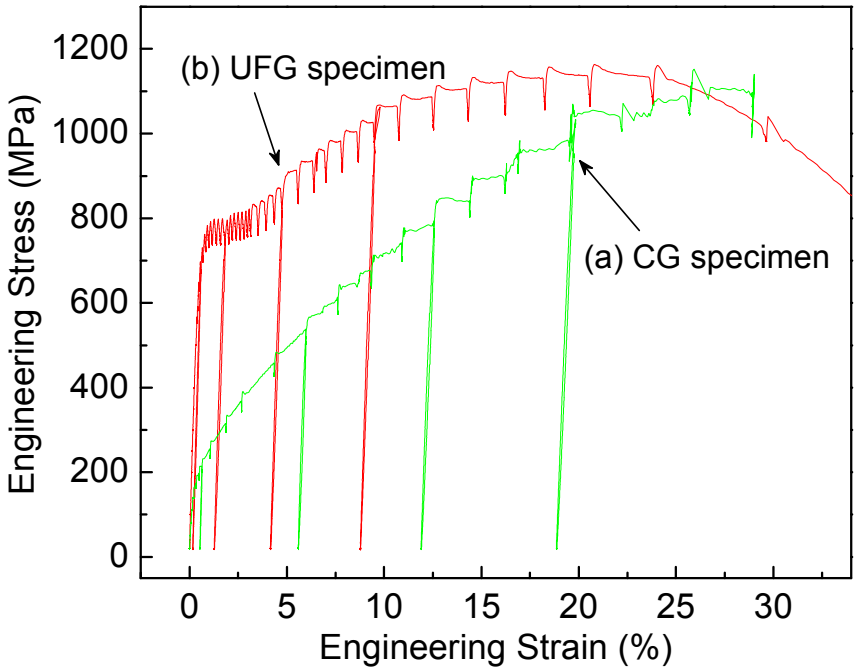

Fig. 1 Tensile engineering stress-strain curves: (a) CG (coarse grained) sample with an average grain size of 50 μm; (b) UFG sample with an average grain size of 350 nm.

shows a yield stress of about 730 MPa, which is dramatically higher than that of the CG specimen (about 210 MPa). On the other hand, the uniform elongation of the UFG specimen (20%) is comparable to that of the CG specimen (25%), that is, the strength is improved markedly without a significant loss of the ductility. In addition, the stress strain curves indicate different transformation behaviors in these two samples. A plateau was observed on the stress-strain curve of the UFG sample, which is believed to be related to the formation of the martensite under relatively constant applied stress. In contrast, the plateau does not appear for the CG sample.

3.2. Martensitic phase transformation

The diffraction spectra were recorded during the tensile tests, showing the process of the transformation. Figs. 2a and b show the axial diffraction patterns (measured with the scattering vector parallel to the loading direction) of the CG and the UFG samples before and after the tensile deformation, respectively. Before deformation, the UFG sample (which had been cold rolled and annealed) has a different texture from that of the CG sample (which shows very weak texture after solution treatment). For instance, the peak intensities of the fcc (220) are quite different in these two samples before deformation.

Fig. 2a shows the axial diffraction patterns of the CG specimen before the tensile deformation and after 25% strain. The reflections from austenite (γ–fcc) and martensite (both α′-bcc and ε–hcp) phases can be clearly observed in the initial diffraction pattern since the martensite start temperature (*Ms*) of the solution treated specimen is higher than room temperature [5]. After 25% strain, which is the end of the uniform elongation under the current experimental condition, the bcc (110) peak grows strong indicating that the bcc martensite (α′) becomes the dominant phase. The austenite phase was almost completely consumed through the transformation. The initially strongest fcc (111) peak can only be found on the shoulder of the bcc (110) peak. Moreover, the intensities of the hcp peaks were also found to decrease at the end of the deformation. In austenitic stainless steel, the martensitic transformation is believed to occur in the sequence of γ → ε → α′ [14]. Therefore, the amount of hcp phase, as an intermediate phase, diminished at the later stage of the transformation. Fig. 2b is the comparison of the diffraction spectra of the UFG specimen before and after 20% strain. Due to the annealing process, most of the martensites (introduced during the cold rolling, which also dropped the *Ms* below room temperature) were reversely transformed to austenite, but a small amount of bcc and hcp phases is still visible. After the tensile deformation of about 20%, the diffraction spectrum is similar to the counterpart of the CG specimen except that the hcp phase is not resolvable in this case.

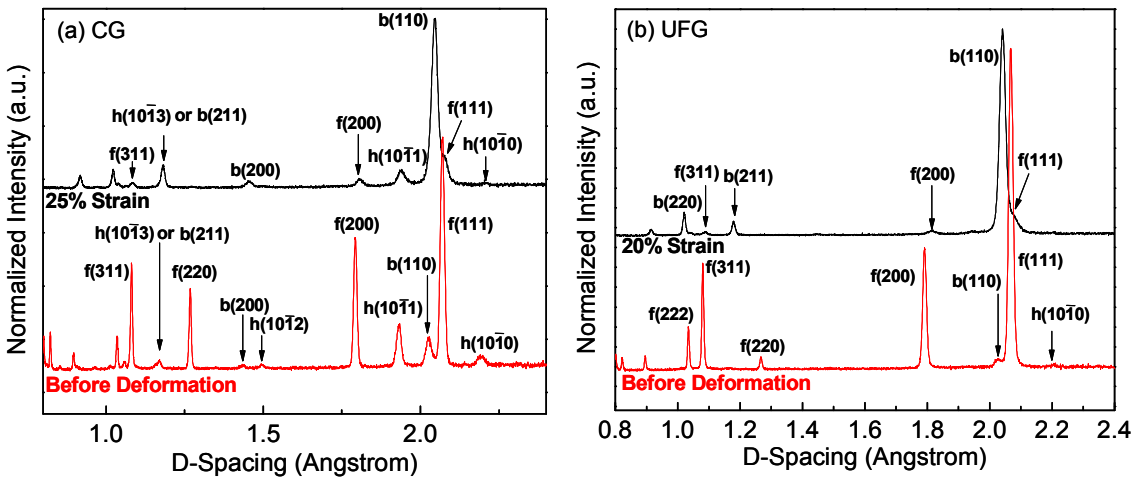

Fig. 2 Axial diffraction spectra before (red) and after deformation (black): (a) CG sample; (b) UFG sample. (Labels: f - fcc austenite, b - bcc martensite, h - hcp martensite)

3.3. Lattice strain evolution in the CG sample and the UFG sample

Fig. 3 shows the axial lattice strain evolution of the CG sample under applied stress. The lattice strain data were calculated using the equation, $\varepsilon=(a-a_0)/a_0$, where a is the lattice parameter under stress and a_0 is the stress-free lattice parameter. The strain responses of the fcc austenite and the hcp martensite (calculated by averaging the strains along a axis and c axis according to $\varepsilon^{hcp} = \frac{1}{3}\left(2\varepsilon_a^{hcp} + \varepsilon_c^{hcp}\right)$) are similar and both deviate from the linearity towards lower lattice strain

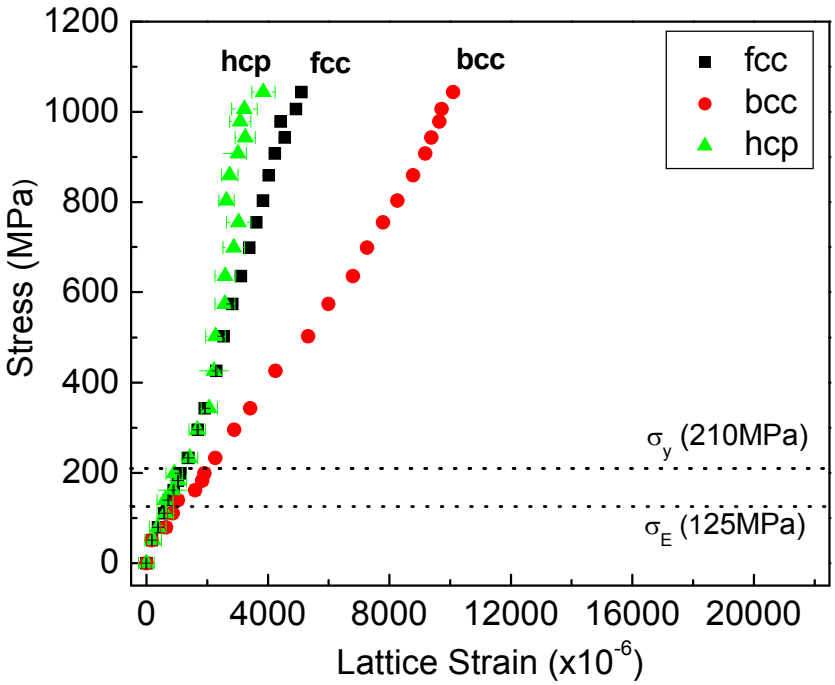

Fig. 3 Evolution of axial lattice strains of the austenite and martensite phases of the CG sample.

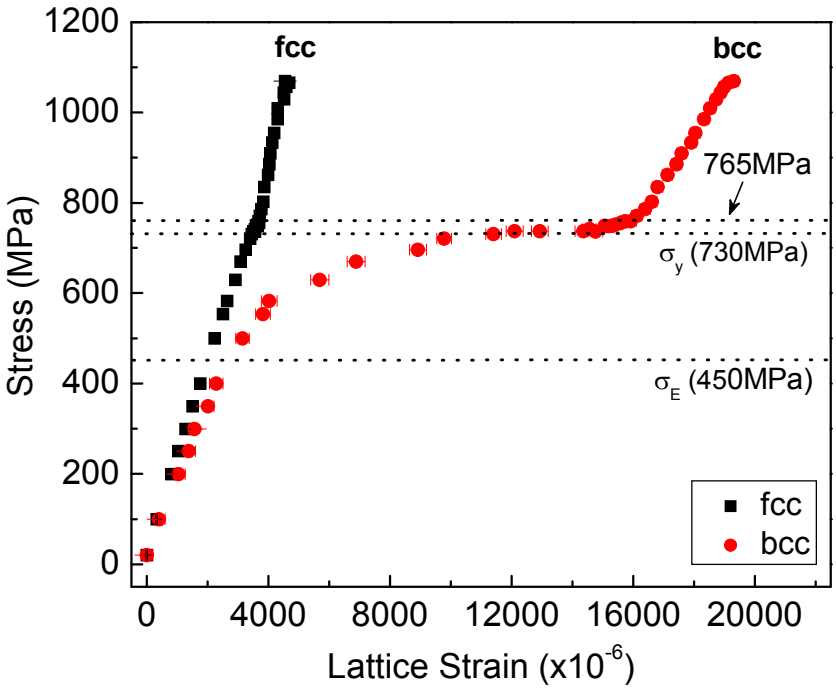

Fig. 4 Evolution of the axial lattice strains of fcc austenite and bcc martensite phases of the UFG sample.

after yielding (above the elastic limit, σ_E), indicating the compressive internal stress developed in these two phases [15]. On the other hand, the bcc martensite deviates to the larger lattice strain and the tensile internal stress is generated in this phase. With the macroscopic applied strain increasing and the phase fraction changing, the bcc martensite carries more of the applied load and plays a role in strengthening.

The axial lattice strain responses of the fcc austenite and the bcc martensite of the UFG specimen are presented in Fig. 4. It is challenging to analyze the accurate phase fraction and lattice strain response of the hcp phase due to its very small amount and broad peak profile. However, the hcp phase was still included in the Rietveld refinement process to ensure the best analysis of the fcc and bcc phases. The lattice strain of the bcc martensite starts to deviate significantly from the linearity when σ_E (about 450 MPa) is reached due to its relatively small starting phase fraction in comparison to the CG specimen. As a result, a large tensile lattice strain developed in the stress range from 450 (elastic limit, σ_E) to about 730 MPa (0.2% yield stress, σ_y). After the martensite formation at the stress level between 730 to 765 MPa, the internal stress development in the martensite starts to slow down since more bcc phase start to share the load. For the austenite phase, the lattice strain remains almost linear until 765 MPa and then, deviates to lower lattice strain when the martensite phase becomes appreciable.

4. Summary

The phase transformation behavior in an ultra-fine-grained (UFG), transformation-induced-plasticity (TRIP) steel was investigated using in situ neutron diffraction. The results of the tensile testing at room temperature and microstrain responses were analyzed. The martensite formation and its interaction with the austenite phase were discussed in the context of the strain hardening and the high ductility maintained in the UFG steel.

Acknowledgements

This work is supported by the NSF International Materials Institutes Program under DMR-0231320. This work has benefited from the use of the Los Alamos Neutron Science Center (LANSCE) at the Los Alamos National Laboratory. LANSCE is funded by the US Department of Energy under Contract W-7405-ENG-36. The authors would like to thank Mr. T. Sisneros and Mr. D. Fielden for their help during the neutron diffraction measurements and sample preparation, respectively.

References

[1]. R.Z. Valiev, R.K. Islamgaliev, and I.V. Alexandrov, Prog. Mater. Sci. Vol. 45 (2000), p. 103.
[2]. Y.T. Zhu, H.G. Jiang, J.Y. Huang, and T.C. Lowe, Metall. Mater. Trans. Vol. 32A (2001), p. 1559.
[3]. Y. Saito, N. Tsuji, H. Utsunomiya, T. Sakai, and R.G. Hong. Scrip. Mater. Vol. 39 (1998), p. 1221.
[4]. Y. Saito, H. Utsunomiya, N. Tsuji, and T. Sakai. Acta Mater Vol. 47 (1999), p. 579.
[5]. E.W. Hart, Acta Met. Vol. 15 (1967), p. 351.
[6]. Y.M. Wang, and E. Ma, Mater. Sci. Eng. A Vol. 375 (2004), p. 46.
[7]. F.D. Fischer, G. Reisner, E. Werner, K. Tanaka, G. Cailletaud, and T. Antretter, Inter. Jour. Plast. Vol. 16(7-8) (2000), p. 723.
[8]. Y.Q. Ma, J.E. Jin, and Y.K. Lee, Scrip. Mater. Vol. 52 (2005), p. 1311.
[9]. Y.Q. Ma, J.E. Jin, and Y.K. Lee, Mater. Sci. For. Vol. 475 (2005), p. 43.
[10]. M.A.M. Bourke, D.C. Dunand, and E. Ustundag, Appl. Phys. A: Mater. Sci. Process. Vol. 74 (2002), p. 1707.
[11]. B. Clausen, T. Lorentzen, M. A. M. Bourke, and M. R. Daymond, Mater. Sci. Eng. A, Vol. 259 (1999), p. 17.
[12]. D. H. Carter and M. A. M. Bourke, Acta Mater, Vol. 48 (2000), p. 2885.

[13]. A.C. Larson and R.B. Von Dreele, GSAS-General Structure Analysis System, Report No. LAUR86-748, 1994.
[14]. K. Spencer, J.D. Embury, K.T. Conlon, M. Veron, and Y. Brechet, Mater. Sci. Eng. A Vol. 387 (2004), p. 873.
[15]. E.C. Oliver, P.J. Withers, M.R. Daymond, S. Ueta, and T. Mori, Appl. Phys. A 74 (2002), p. 1143.